

## RESEARCH ARTICLE

# Structural behavior of RC columns retrofitted with FRP under axial load

Ali Juma Noorzad<sup>1\*</sup>, Hakan Dilmaç<sup>2</sup>

- <sup>1</sup> Suleyman Demirel University, Graduate School of Natural and Applied Sciences, Isparta, Türkiye
- <sup>2</sup> Suleyman Demirel University, Faculty of Engineering and Natural Sciences, Isparta, Türkiye

## **Article History**

Received 2 December 2024 Accepted 2 January 2025

#### **Keywords**

Axial strength FRP TSR RC column Retrofitted Ductility Stress-strain

#### **Abstract**

The strengthening of reinforced concrete columns using fiber-reinforced polymer (FRP) composites has garnered significant attention in recent years due to its numerous advantages. RC columns primarily support axial compression loads and often require strengthening to improve their axial strength and ductility. This research investigates the analytical structural axial behavior of rectangular RC columns retrofitted externally with FRP, internally strengthened with transverse steel reinforcement (TSR), or strengthened using a combination of FRP and TSR techniques, applied externally and internally, respectively. The research also aims to identify precise stress-strain models that accurately represent the mechanical behavior of rectangular RC columns which experience irregular stress variations due to their geometry, in three different confinement configurations: FRP, TSR, and combined confinement of FRP and TSR, under pure axial compression loads. Furthermore, five rectangular and square cross-sectional RC columns with various dimensions and confinement configurations have been analyzed using three confinement methods under pure axial compressive load, and all influential parameters were investigated analytically with the proposed models. The results show that the stress-strain relationships obtained from the suggested models are in good agreement with experimental data taken from the literature and previous studies. Based on the findings, combined confinement reinforcement using FRP and TSR demonstrates greater benefits than individual methods in improving the structural axial behavior of rectangular RC columns under axial loads, making this technique particularly effective for enhancing axial load-bearing capacity and ductility.

#### 1. Introduction

In the past few years, Fiber Reinforced Polymer (FRP) materials have been developed consistently popular for strengthening the durability of reinforced concrete structures, especially in cases involving aging, load carrying capacity, or environmental damage. This retrofitting method provides several benefits over traditional techniques, including high strength-to-weight ratios, resistance to corrosion, and ease of installation. Carbon Fiber Reinforced Polymer (CFRP) wraps have proven to be a highly effective option for

eISSN 2630-5763 © 2023 Authors. Publishing services by golden light publishing®.

<sup>\*</sup> Corresponding author (<u>alijumanoorzad@gmail.com</u>)

This is an open-access article under the CC BY-NC-ND license (http://creativecommons.org/licenses/by-nc-nd/4.0/).

strengthening the structural performance of RC columns under axial or centric loads [1]. The enhancement of axial capacity in plain concrete columns reinforced with FRP fabrics has been extensively investigated through both analytical and experimental methods. However, research on reinforced concrete columns strengthened with FRP and TSR remains relatively limited. Since FRP jackets are an effective solution for upgrading deficient reinforced concrete columns in older buildings located in seismic regions. This study focuses on axially loaded RC columns with rectangular cross-sections that externally fully wrapped along their lengths with carbon fiber reinforced polymer (CFRP) and internally confined with stirrups (TSR) [2]. This study reviews the fundamental assumptions used in analytical models for estimating the stress-strain relationships, lateral confining pressures, peak values of stress and strain, and nominal axial loads of rectangular RC columns under various confinement conditions. A straightforward design model is introduced and thoroughly detailed, developed by combining ACI-440.2R provisions to ensure accurate and safe predictions. Additionally, four models from the literature chosen for their strong alignment with experimental data are presented, and specific features of these models are discussed [3, 4].

In the past, numerous studies have investigated FRP-reinforced concrete columns. One notable example is the Lam and Teng model, which proposed a stress-strain relationship for reinforced concrete columns retrofitted with FRP jackets. This model has demonstrated acceptable accuracy in predicting the stress-strain curve, lateral confining pressure, and confined compressive strength and strain of concrete for various crosssectional shapes, including circular and rectangular sections. Furthermore, the ACI 440.2R guidelines adopt this model for calculating the strength of FRP-strengthened columns [5, 6]. Afifi et al. [7] proposed a confinement model for RC columns externally confined with FRP and internally reinforced with TSR. The model effectively predicts the stress-strain behavior of column cross-sections under pure axial load. To validate this model, axial compression tests were conducted on 72 concrete columns confined with FRP and stirrups, incorporating varying cross-sectional shapes and corner radii. The study introduced accurate models for the stress-strain relationship and the coordinates of the peak and ultimate points under axial loading. Wei et al. [8] investigated the combined FRP/TSR model for rectangular reinforced concrete columns. This model considers the stress-strain diagrams for both the concrete core and the cover. The results showed good agreement with the experimental data. Samaan et al. [9] proposed an empirical model to predict the behavior of concrete columns that are exclusively confined with FRP tubes. Mirmiran et al. [10] applied the same equation to determine the compressive strength of confined concrete ( $f_{cc}$ ) in columns wrapped with FRP. In the 2008 document ACI 440.2R-08 [11], the ACI committee 440 outlines procedures for developing the interaction diagram for reinforced concrete columns wrapped with FRP and they specified certain limitations for components subjected to both axial compression and bending. Notably, the effective strain in the FRP jacket must not surpass a designated value derived from their proposed equation. This constraint is established to maintain the shear integrity of the confined concrete [5]. Rami and Paultre [12] investigated the compressive behavior of FRP-confined reinforced concrete columns under axial loading. They studied the structural behavior of RC columns that were confined externally with FRP jackets and internally with transverse steel reinforcement (TSR) both analytically and experimentally for circular, square, and rectangular cross-sections. They developed a unified stress-strain model based on the axial behavior of RC columns with various cross-sections. Additionally, they conducted experiments on six FRP/TSR-confined square RC columns under compressive loading and plotted the axial stress-strain curve experimentally, subsequently comparing the results with analytical studies [13].

This study focused on rectangular RC columns confined simultaneously with FRP and TSR and subjected to concentric compression loads. The primary objective is to investigate the actual compression behavior of rectangular columns with varying geometric properties under three types of confinement: TSR, FRP, and combined TSR/FRP. For all confinement configurations, the structural parameters of the columns were analyzed, and the results were compared with experimental data obtained from previous studies cited in the

literature. This research addresses a gap in the existing literature and provides a comprehensive reference for the analysis of confined RC columns under axial loads.

#### 2. Material and method

#### 2.1. Material

FRP reinforced columns are composed of three materials: plain concrete, steel reinforcement, and fiber polymer reinforcement, each possessing distinct mechanical and physical properties. Concrete is a complex composite material with high compressive strength but low tensile strength. To address this limitation, steel reinforcement is used in tensile zone of reinforced concrete structures. Understanding the compressive strength of concrete is crucial for the analysis and design of RC structures. Its value varies based on the combination of primary materials, such as aggregates, cement, and, in some cases, admixtures properties. For the analysis of column cross-sections in this study, normal-weight concrete with a compressive strength of 25 MPa is used. The elastic modulus of concrete is frequently utilized for reinforced concrete members strengthened with FRP. According to ACI 318-08, the elastic modulus of concrete can be determined using the following expression [11].

$$E_c = 4700\sqrt{f_c'} \quad [MPa] \tag{1}$$

Steel reinforcement is used in reinforced concrete structures as a tensile material, providing strength, ductility, and stability. Steel reinforcements are placed in the tensile zones of concrete structures to address the lack of tensile strength in concrete. In reinforced concrete columns, two types of steel reinforcement are used: longitudinal steel bars and transverse steel reinforcement (stirrups). Both play essential roles in the stress-strain relationships and load capacity of RC columns. For the parametric study of a column's cross-section, the modulus of elasticity for steel is frequently used, with a typical value of 200 GPa for mild or structural steel.

Carbon fiber reinforced polymer (CFRP) is a composite material made by reinforcing a plastic polymer. This material provides sufficient strength, rigidity, and lightness for reinforced concrete structures. Its high tensile strength, high modulus of elasticity, and high strength-to-weight ratio are among the advantages of this composite material. FRP is classified into various types based on its physical and mechanical properties; in this study, a CFRP jacket is used. The modulus of elasticity of FRP is not constant and depends on its components [1].

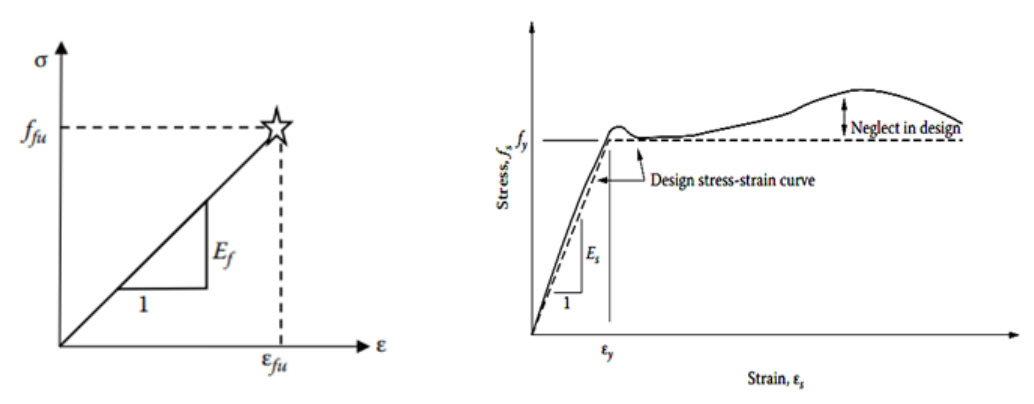


Fig. 1. Stress-strain behavior of FRP and steel reinforcement [13]

RC columns with FRP consist of concrete, steel reinforcement, and fiber polymer reinforcement, each having unique mechanical properties. The materials used for the parametric analysis in this research include plain concrete with normal weight or Type I Portland cement, mild structural steel reinforcement with a yield tensile strength of 420 MPa for both longitudinal bars and transverse steel reinforcement (stirrups), and carbon fiber reinforcement with an elastic modulus of 230 GPa and an ultimate tensile strain of 0.018. Fig. 1 illustrates the structural and mechanical strength of concrete, steel reinforcement, and FRP reinforcement under compression and tensile loads.

#### 2.2. Method

This study aims to predict the analytical axial compressive behavior of rectangular RC columns strengthened with FRP and TSR by evaluating several proposed models. Established models from the literature, such as the Lam and Teng model and the Mander et al. [14] model, were selected to analyze the column's cross-sections under axial loads. The results of parametric studies were then compared with experimental data to assess their accuracy. To enhance understanding, three RC columns with rectangular and square cross-sections were analytically evaluated under axial compression loads. These evaluations considered three confinement configurations: TSR confinement with varying stirrup spacing, FRP confinement with different thicknesses and corner radii, and a combined TSR/FRP configuration incorporating variations in spacing, thickness, and corner radii. The results of these analyses are presented in tables and graphs for clarity. Key parameters critical to the performance of confined RC columns include lateral confining pressures, peak and maximum confined compressive strength and strain of concrete, strength and ductility ratios of the cross-section, and the theoretical axial load capacity of the column. These parameters have been extensively studied using reliable analytical models for RC columns subjected to concentric compression loads. Additionally, numerous experimental specimens from the literature were analyzed for comparison, with all parameters calculated using the proposed models.

## 3. Analytical models

## 3.1. Confinement models for FRP wraps exclusively

Lam and Teng [6] proposed a stress-strain relationship model for reinforced concrete columns strengthened with FRP jackets, which has been adopted by ACI 440.2R for the analysis of FRP-RC columns. Their results showed that this model provides the most accurate and reliable predictions for the confined compressive strength of concrete in both circular and rectangular columns [5, 6, 13]. Based on this model, confining rectangular columns with FRP wraps can provide a marginal increase in the peak confined concrete strength fc. The provisions of this model are not recommended for members with side aspect ratios h/b greater than 2.0 or face dimensions b or h exceeding 900 mm. Furthermore, this model investigates the strength and ductility of RC columns retrofitted with FRP confinement only and does not consider TSR or a combination of FRP and TSR. The corresponding equations for this model are as follows:

$$f_c = \begin{cases} E_c \varepsilon_c - \frac{(E_c - E_2)^2}{4f_c'} \varepsilon_c^2 \Rightarrow 0 \le \varepsilon_c \le \varepsilon_t \\ f_c' + E_2 \varepsilon_c \Rightarrow \varepsilon_t < \varepsilon_c \le \varepsilon_{ccu} \end{cases}$$
 (2)

$$E_2 = \frac{f_{cc} - f_c'}{\varepsilon_{ccu}} \tag{3}$$

$$\varepsilon_t = \frac{2f_c'}{E_c - E_2} \tag{4}$$

$$f_{cc} = f'_c + \psi_f \times 3.3 \times k_a \times f_l \qquad \psi_f = \begin{cases} 1 & [6] \\ 0.95 & [11] \end{cases}$$
 (5)

$$f_l = \frac{2nt_f E_f \varepsilon_{fe}}{D} \tag{6}$$

where is  $f_c$  is the longitudinal axial stress,  $\varepsilon_c$  longitudinal axial strain of sections,  $E_c$  elastic modulus of concrete (based on ACI-318,  $E_c = 4700\sqrt{f_c'}$  MPa for normal weight of concrete)  $f_{cc}$  is confined compressive strength of concrete,  $\varepsilon_{cc}$  confined strain of concrete, n the number of FRP layers,  $t_f$  thickness of FRP,  $f_l$  lateral confining pressure, D the equivalent diameter of cross sections,  $\psi_f = 0.95$  is an additional reduction factor propose by ACI 440.2R-08,  $k_a$  is a strength efficiency factor which account for the section geometry ( $k_a = 1$  for a circular section and while its computation for a non-circular sections obtained from a specific equation), and  $\varepsilon_{fe} = k_{\varepsilon}\varepsilon_{fu} = 0.586\varepsilon_{fu}$  as averaged by Lam and Teng [6]. According to this model, the minimum confinement ratio ( $f_l/f_{co}$ ) should be larger than 0.07 for confined axial stress-strain diagram or circular columns. For non-circular sections, the ratio ( $f_l/f_{co}$ ) is multiplied by  $k_a = 1$  with the product exceeding 0.07 to have an ascending second branch. Fig. 2 shows the stress-strain curves of the Lam and Teng model at different loading stages. The initial stage of the graph follows a parabolic shape, with its slope corresponding to the elastic modulus of concrete ( $E_c$ ). The second part of the graph is linear, starting at the transition strain ( $\varepsilon_t$ ) and continues up to the maximum strain ( $\varepsilon_c$ ).

For rectangular cross-sections, Lam and Teng suggested additional shape factors  $k_a$  and  $k_b$ . They also transformed the rectangular section into an equivalent circular section, as illustrated in Fig. 3. The equivalent section and shape factors are determined using the following equations.

$$D = \sqrt{b^2 + h^2} \tag{7}$$

$$k_a = \frac{A_e}{A_c} \left(\frac{b}{h}\right)^2 \tag{8}$$

$$k_b = \frac{A_e}{A_c} \left(\frac{h}{b}\right)^{0.5} \tag{9}$$

$$f_l = \frac{2E_f n t_f \varepsilon_{fe}}{\sqrt{h^2 + h^2}} \tag{10}$$

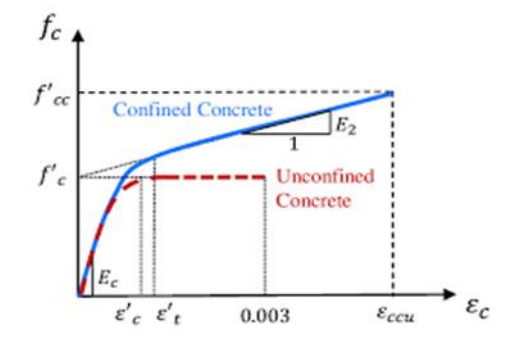


Fig. 2. Lam and Teng [6] model for FRP-confined columns

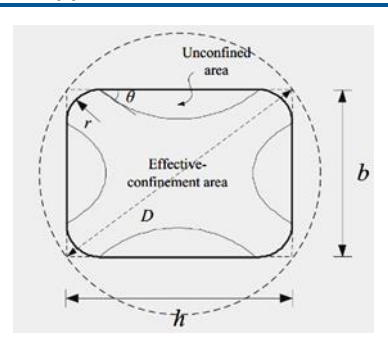


Fig. 3. Effective area of confined rectangular column [13]

Based on ACI 440.2R-08 the effectively confined area of concrete was presumed to be represented by parabolas, with an initial slope matching that of the adjacent diagonal. The confined area ratio or confinement efficiency factor is calculated using the following equation.

$$\frac{A_e}{A_c} = \frac{1 - \frac{\left[ \left( \frac{b}{h} \right) (h - 2r_c)^2 + \left( \frac{h}{b} \right) (b - 2r_c)^2 \right]}{3A_g} - \rho_g}{1 - \rho_g} \tag{11}$$

where  $A_e$  represents the effective area of confined concrete,  $A_c$  is the area of the concrete core,  $A_g$  is the gross area of the section,  $\mathcal{F}_g$  is the steel percentage of longitudinal bars,  $R_c$  is the radius of the corner of the rectangular section, and b and h are the dimensions of the cross-section. Lam and Teng [6] suggested the following equation for the ultimate strain.

$$\varepsilon_{ccu} = \varepsilon_c \left( A + 12k_b \frac{f_l}{f_c} \left( \frac{\varepsilon_{fe}}{\varepsilon_c} \right)^{0.45} \right) \le 0.01 \qquad A = \begin{cases} 1.75 & [6] \\ 1.5 & [11] \end{cases}$$
 (12)

where  $k_b$  is a strain efficiency factor to account for the section geometry  $k_b = 1$  for circular cross sections and  $k_b$  rectangular sections based on ACI 440.2R-08.

Richart et al. [15] model is one of the reliable models used to investigate the structural behavior of confined concrete, particularly under the influence of transverse steel reinforcement. It was originally developed for steel-confined concrete with continuous lateral reinforcement. However, many researchers have also applied it to FRP confinement. Despite its goodness, this model has several limitations, such as: it does not consider FRP rupture or the sudden loss of confinement, it ignores the interaction between FRP wraps and steel reinforcement, and its accuracy is limited for high-strength concrete. Richart et al. [15] proposed a model for estimating the peak confined axial strain ( $\varepsilon_{cc}$ ) at the maximum confined compressive strength of concrete ( $f_{cc}$ ). This model considers the unconfined axial strain ( $\varepsilon_{co}$ ) at the maximum unconfined compressive strength of concrete ( $f_{co}$ ), along with the lateral confining pressure and the confinement effectiveness factor. In their experiments, Richart used concrete specimens confined with active hydrostatic fluid pressure.

$$f_{cc} = f_{co} + k_1 f_1 \tag{13}$$

$$\varepsilon_{cc} = \varepsilon_o (1 + k_2 f_l / f_{co}) \tag{14}$$

where  $f_{cc}$ ,  $\varepsilon_{cc}$  are the confined compressive strength and strain of concrete,  $f_{co}$ ,  $\varepsilon_{o}$  are the compressive strength and strain of unconfined concrete;  $f_{l}$  is the lateral hydrostatic pressure;  $k_{1} = 4.1$ , and  $k_{2} = 5k_{1}$ . Furthermore, reliable analytical stress-strain models for rectangular RC columns strengthened with FRP and TSR are shown in Table 1. The expressions for stress, strain, and stress-strain relationships are illustrated consistently.

## 3.2. Confinement of rectangular RC column with TSR

Mander et al. [14] developed a unified stress-strain model for reinforced concrete members confined with transverse steel reinforcement (TSR) or stirrups. This model accounts for the effect of stirrups on lateral confining pressure (which may be either equal or unequal), as well as the confined compressive strength and strain of the concrete. It can be used for members subjected to both static and dynamic loads, whether applied monotonically or cyclically, and is suitable for both circular and rectangular cross-sections [17, 18]. Despite its advantages, this model has some limitations, such as: it is not suitable for cyclic or seismic loading conditions, it overestimates the compressive strength and ductility of RC columns with high-strength concrete, and it is inaccurate for non-axially loaded columns.

Mander et al. [14] proposed the following expressions for evaluating the stress-strain curves of reinforced concrete cross-sections.

$$f_c = \frac{f_{cc}xr}{r - 1 + x^r} \tag{15}$$

$$x = \frac{\varepsilon_c}{\varepsilon_{cc}} \tag{16}$$

$$r = \frac{E_c}{E_c - E_{sec}} \tag{17}$$

$$E_{sec} = \frac{f_{cc}}{\varepsilon_{cc}} \tag{18}$$

where  $f_c$  and  $\epsilon_c$  are the longitudinal compressive stress and strain for concrete, and  $f_{ccf}$  and  $\epsilon_{cc}$  are the peak confined compressive strength and strain of concrete, and  $f_c$  and  $\epsilon_{co}$  are the unconfined compressive strength and strain of concrete, respectively.

A unified stress-strain relationship was developed by Mander et al. [14] for RC members strengthened with TSR, and the correlation between stress and strain is illustrated (Fig. 4). The confined concrete curve represents the behavior of RC columns subjected to pure axial load. The first (ascending) branch starts with a slope corresponding to the elastic modulus of concrete ( $E_c$ ), which decreases as the stress rises, eventually reaching its peak value, known as the confined compressive strength of concrete ( $f_{cc}$ ). The second (descending) branch illustrates the ductile region of the curve.

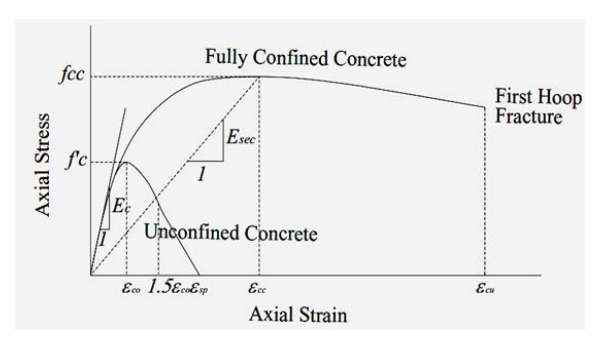


Fig. 4. Stress-strain curves for confined concrete with TSR (Mander et al. [14])

Table 1. Analytical models for FRP and TSR confinement

Model	Ultimate stress	Ultimate strain	Stress-strain relationship
Harajli et al. [19]	$\frac{f_{cu}}{f_{co}} = 1 + 1.25 \left( \frac{f_{lfe} + f_{lse}(A_{cc}/A_g)}{f_{co}} \right)^{-0.5}$	$\frac{\varepsilon_{cu}}{\varepsilon_{co}} = \left[ \left( \frac{25800e^{1.17b/h}}{\left( \rho_f E_f \right)^{0.83}} \right) \varepsilon_l + 2.0 \right] \left( \frac{f_{cu}}{f_{co}} - 1 \right)$	$\begin{cases} f_c = f_o \left[ \frac{2\varepsilon_c}{\varepsilon_o} - \left( \frac{\varepsilon_c}{\varepsilon_o} \right)^2 \right] \\ f_c = \sqrt{(K_o - K)} - K_o \end{cases}$ $f_o = f_{co} + k \left[ f_{lfe} + f_{lse} \left( \frac{A_{cc}}{A_g} \right) \right]$ $\varepsilon_o = \varepsilon_{co} \left[ 1 + (310.57\varepsilon_{lo} + 1.9) \left( \frac{f_o}{f_{co}} - 1 \right) \right]$
Samaan et al. [9]	$f_{cu} = f_{co} + 6.0 f_{lf}^{0.7} [MPa]$	$\varepsilon_{cu} = \frac{f_{cu} - f_o}{E_2}$ $f_o = 0.872 f_{co} + 0.371 f_{lf} + 6.258 [MPa]$ $E_2 = 245.61 f_{co}^{0.2} + 1.3456 \frac{E_f + t_f}{D} [MPa]$	$f_c = \frac{(E_1 - E_2)\varepsilon_c}{\left[1 + \left(\frac{(E_1 - E_2)\varepsilon_c}{f_o}\right)^n\right]^{\frac{1}{n}}} + E_2\varepsilon_c$ $E_1 = 3950\sqrt{f_{co}} [MPa]$

Faustino et al. [20] 
$$f_{cu} = f_{co} + 3.7 \left(\frac{2r}{b}\right) f_l$$
 
$$\varepsilon_{cu} = 18.89 \varepsilon_{co} \left(\frac{f_l}{f_{co}}\right)$$
 
$$f_c = \frac{(E_o - E_1)\varepsilon_c}{\left[1 + \left(\frac{(E_o - E_1)\varepsilon_c}{f_l}\right)^n\right]^{\frac{1}{n}}} + E_1 \varepsilon_c \le f_{cu}$$

DD 1			~		
Tab	le	١. ١	Co	ntı	nued

Model Ultimate stress Ultimate strain Stress-strain relationship

$$\begin{bmatrix} \frac{f_{cu}}{f_{co}} - 1 \end{bmatrix}_T = \begin{bmatrix} \frac{f_{cu}}{f_{co}} - 1 \end{bmatrix}_{FRP} + \begin{bmatrix} \frac{f_{cu}}{f_{co}} - 1 \end{bmatrix}_{TSR} \qquad \begin{bmatrix} \frac{\varepsilon_{cu}}{\varepsilon_{co}} - 1 \end{bmatrix}_{TOTAL} = \begin{bmatrix} \frac{\varepsilon_{cu}}{\varepsilon_{co}} - 1 \end{bmatrix}_{FRP} + \begin{bmatrix} \frac{\varepsilon_{cu}}{\varepsilon_{co}} - 1 \end{bmatrix}_{TSR}$$
 Ilki et al. 
$$\begin{bmatrix} \frac{f_{cu}}{f_{co}} \end{bmatrix}_{FRP} = \begin{bmatrix} 1 + 2.54 \left( \frac{f_{lfe}}{f_{co}} \right) \end{bmatrix} \qquad \qquad \begin{bmatrix} \frac{\varepsilon_{cu}}{\varepsilon_{co}} \end{bmatrix}_{FRP} = \begin{bmatrix} 1 + 19.27 \left( \frac{b}{h} \right) \left( \frac{f_{lfe}}{f_{co}} \right)^{0.53} \end{bmatrix}$$
 
$$\begin{bmatrix} \frac{f_{cu}}{f_{co}} \end{bmatrix}_{TSR} = \begin{bmatrix} 1 + 4.54 \left( \frac{f_{lse}}{f_{co}} \right) \end{bmatrix} \qquad \qquad \begin{bmatrix} \frac{\varepsilon_{cu}}{\varepsilon_{co}} \end{bmatrix}_{TSR} = \begin{bmatrix} 1 + 5 \left( \left( \frac{f_{cu}}{f_{co}} \right)_{TSR} - 1 \right) \end{bmatrix}$$

$$\begin{split} \frac{f_{cu}}{f_{co}} &= 1 + k_1 \left(\frac{f_{le}}{f_{co}}\right)^{1-\alpha} \\ k_1 &= k_A \cdot k_R \\ k_A &= A \left(\frac{f_{le}}{f_{co}}\right)^{-\alpha} \\ \begin{cases} k_R &= 1 - 2.5(0.3 - 2r/b) \rightarrow 2r/b < 0.3 \\ k_R &= 1 \rightarrow 2r/b \ge 0.3 \end{split}$$

$$\frac{\varepsilon_{cu}}{\varepsilon_{co}} = 2 + B \frac{f_{le}}{f_{co}}$$

$$f_c = \frac{(E_o - E_1)\varepsilon_c}{\left[1 + \left(\frac{(E_o - E_1)\varepsilon_c}{f_l}\right)^n\right]^{\frac{1}{n}}} + E_1\varepsilon_c$$

Noorzad and Dilmaç

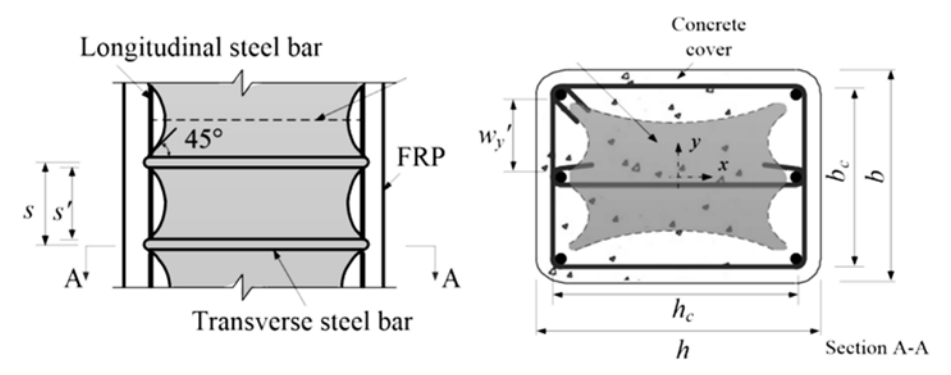


Fig. 5. Core of rectangular TSR with effective confinement (Mander et al. [14])

The areas of effective confinement in rectangular reinforced concrete columns confined with TSR are shown (Fig. 5). The arching effect is modeled as parabolas with an initial angle of 45°, occurring vertically between layers of TSR and horizontally between the longitudinal steel reinforcements. In addition, Fig. 5 illustrates that the effectively confined region is smaller than the core area. As a result, the effective lateral confining pressure (F'L) is determined as a percentage of the lateral confining pressure from the TSR (FL), as demonstrated below:

$$f_l' = k_e \times f_l \tag{19}$$

$$k_e = \frac{A_e}{A_{cc}} \tag{20}$$

$$A_{cc} = A_c (1 - \rho_{cc}) \tag{21}$$

where  $k_e$  is the confinement effectiveness factor,  $A_e$  is the effective area of the concrete core, and  $\mathcal{F}_{cc}$  represents the steel percentage of longitudinal bars relative to the core area. The effective area of the concrete core is calculated by excluding the areas of the horizontal and vertical parabolas illustrated in Fig. 5. The formula for determining the effective area  $(A_e)$  is as follows:

$$A_e = \left(b_c h_c - \sum_{i=1}^n \frac{{w_i}^2}{6}\right) \left(1 - \frac{s'}{2b_c}\right) \left(1 - \frac{s'}{2h_c}\right)$$
 (22)

where,  $w_i$  represents the clear spacing between the i-th pair of adjacent longitudinal steel reinforcement, and n is the total number of longitudinal steel bars. Substituting these values into the equation for the confinement effectiveness factor the following expression will be obtained:

$$k_{e} = \left(1 - \sum \frac{w_{i}^{2}}{6b_{c} \times h_{c}}\right) \left(\frac{\left(1 - \frac{s'}{2b_{c}}\right)\left(1 - \frac{s'}{2h_{c}}\right)}{1 - \rho_{cc}}\right)$$
(23)

$$k_e = k_v \times k_h \ge 0 \tag{24}$$

$$k_{v} = \frac{\left(1 - \frac{s'}{2b_{c}}\right)\left(1 - \frac{s'}{2h_{c}}\right)}{1 - \rho_{cc}} \ge 0 \tag{25}$$

$$k_h = \left(1 - \sum \frac{w_i^2}{6b_c \times h_c}\right) \ge 0 \tag{26}$$

$$\rho_{cc} = \frac{\sum A_{st}}{b_c \times h_c} \tag{27}$$

The steel percentages in each transverse direction are determined as follows:

$$\rho_x = \frac{\sum A_{tx}}{s \times h_c} \tag{28}$$

$$\rho_y = \frac{\sum A_{ty}}{s \times b_c} \tag{29}$$

The lateral confining pressures can be calculated using the following equations:

$$f_{lx} = f_{ys} \times \frac{\sum A_{stx}}{s \times h_c} = f_{ys} \times \rho_x \tag{30}$$

$$f_{ly} = f_{ys} \times \frac{\sum A_{ty}}{s \times b_c} = f_{ys} \times \rho_y \tag{31}$$

Subsequently, the effective confined pressures are determined as follows:

$$f'_{lx} = k_e \times f_{lx} \tag{32}$$

$$f'_{ly} = k_e \times f_{ly} \tag{33}$$

$$f'_{l} = 0.5(f'_{lx} + f'_{ly}) \tag{34}$$

The peak confined compressive strength of concrete for RC columns confined with TSR is calculated using the following equation adopted from Mander et al. [14].

$$f_{cc} = \alpha f_{co} \left[ 2.254 \sqrt{1 + \frac{7.94f'_l}{f_{co}}} - \frac{2f'_l}{f_{co}} - 1.254 \right]$$
 (35)

The value of  $\alpha$  is 1 for CFRP and 1.12 for GFRP, regardless of the number of strands.

The peak strain at which the confined concrete reaches its ultimate value in reinforced concrete members enclosed by the TSR method is obtained using the following equation suggested by Richart et al. [15].

$$\varepsilon_{cc} = \varepsilon_{co} \left[ 1 + 5 \left( \frac{f_{cc}}{f_{co}} - 1 \right) \right] \tag{36}$$

The maximum strain at which the confined concrete reaches its failure point is obtained using the following expressions:

$$\varepsilon_{cu} = 0.004 + 0.1\rho_s \frac{f_y}{f_{co}} \tag{37}$$

#### 3.3. Combined confinement using FRP wraps and TSR

As discussed previously, Mander et al. [14] model was developed specifically for RC columns confined only with TSR, while the Lam and Teng model was formulated for RC columns confined solely with FRP wraps.

In practical applications, however, RC columns are often confined using a combination of TSR and FRP jackets or are subjected to different lateral confining pressures from both stirrups and fiber-reinforced polymer wraps. To investigate the interaction between these two confinement methods, a new model has been introduced to evaluate the combined structural behavior of RC columns under dual confinement. This proposed model incorporates the effects of both TSR and FRP, as explored in the Mander and Lam and Teng models and provides a method to predict the stress-strain curves, lateral confining pressures, and peak stress-strain coordinates of RC columns confined with TSR and FRP wraps simultaneously. The expression for lateral confinement is modified to include two lateral confining pressures in the x- and y-directions [4, 12]. This formulation considers the contributions of both TSR and FRP wraps within the core ( $f_{le}$ ) and FRP wraps alone in the cover region of the core ( $f_{lf}$ ), as illustrated in Fig. 5. The corresponding expressions are as follows:

$$f_{lxf} = k_f \frac{2n_f E_f t_f \varepsilon_{fe}}{h} \tag{38}$$

$$f_{lyf} = k_f \frac{2n_f E_f t_f \varepsilon_{fe}}{b} \tag{39}$$

$$f_{lxe} = k_f \frac{2n_f E_f t_f \varepsilon_{fe}}{h} + k_e \rho_x f_{ys}$$
(40)

$$f_{lye} = k_f \frac{2n_f E_f t_f \varepsilon_{fe}}{b} + k_e \rho_y f_{ys}$$
(41)

$$k_{f} = \frac{A_{e}}{A_{c}} = \frac{1 - \frac{\left[\left(\frac{b}{h}\right)(h - 2r_{c})^{2} + \left(\frac{h}{b}\right)(b - 2r_{c})^{2}\right]}{3A_{g}} - \rho_{g}}{1 - \rho_{g}}$$
(42)

$$k_{e} = \left(1 - \sum \frac{w_{i}^{2}}{6b_{c} \times d_{c}}\right) \left(\frac{\left(1 - \frac{s'}{2b_{c}}\right)\left(1 - \frac{s'}{2d_{c}}\right)}{1 - \rho_{cc}}\right)$$
(43)

Within the structure of the combined confinement model for FRP and TSR, the choice of an appropriate model, such as Lam and Teng or Mander, depends on the confinement ratio determined by the FRP. When the confinement ratio  $(f_{\rm lf}/f_{\rm co})$  exceeds 0.08, the ascending second branch is activated, and the Lam and Teng model is suggested to compute stress-strain curves, the confined compressive strength of concrete, and other cross-sectional parameters for both the core and cover. On the other hand, if the confinement ratio  $(f_{\rm lf}/f_{\rm co})$  falls below 0.08, the Mander model is applied for these computations. The confinement ratio limit of 0.08 is specified by ACI 440.2R.

Once the parameters of the selected model are determined, stresses are calculated using the equations of the applied model for both the core and the cover. Since the cover typically exhibits a lower ultimate strain due to reduced confinement pressure, there are instances where the cover stress drops to zero at certain strain levels, while the core remains active and intact. This situation is unrealistic because the presence of FRP prevents the spalling of the concrete cover. To resolve this, it is assumed that the stress-strain curve remains constant beyond the ultimate strain. When the cover's ultimate strain is exceeded, the cover stress remains fixed at that value until the core's ultimate strain is reached. This adjustment is applicable only to cases involving the Lam and Teng model [6].

The stress-strain curves are shown in Fig. 8. for confined concrete in the core and cover of the column cross-section, strengthened with combined confinement using FRP wraps and TSR under axial compressive loads, based on the models by Mander et al. [14] and Lam and Teng [6], respectively. According to the stress-strain curves, the peak confinement stress and strain of the concrete differ between the two models and depend on the confinement ratio. These values are determined using a 3D stress state, which will be discussed in the next section.

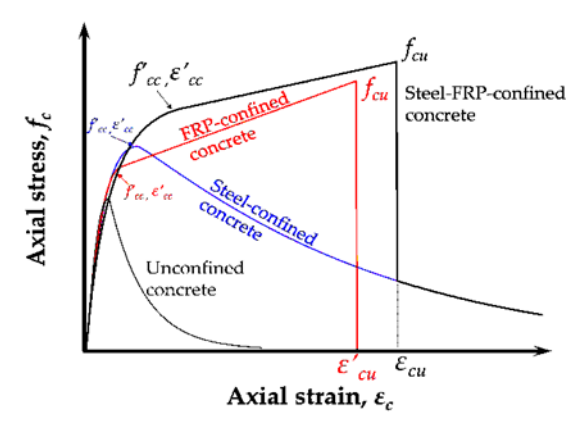


Fig. 6. Suggested stress-strain curves for columns confined with FRP and TSR

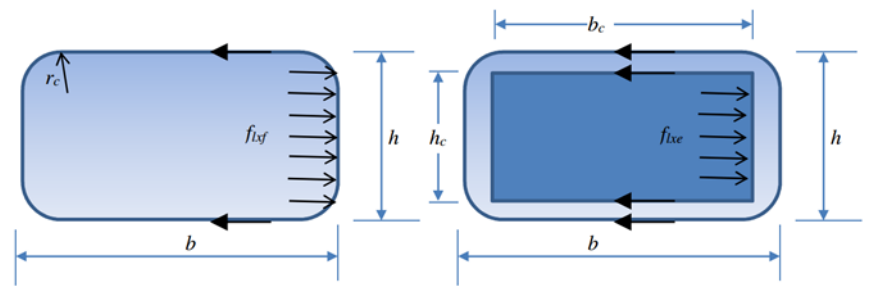


Fig. 7. Effective pressure of the confined rectangular column [4]

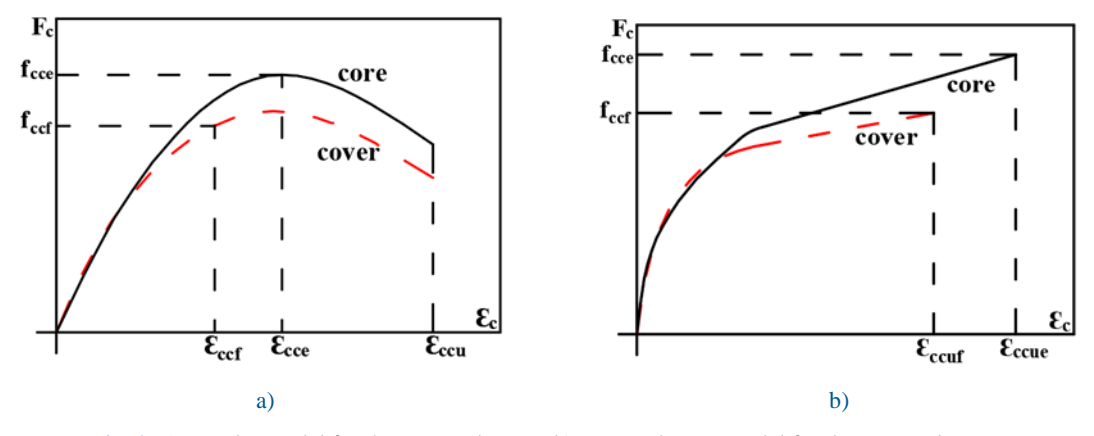


Fig. 8. a) Mander model for the core and cover, b) Lam and Teng model for the core and cover

# 3.3.1. Peak compressive strength of concrete confined by FRP and TSR

The maximum confined strength values of the concrete core and cover ( $f_{cce}$ ,  $f_{ccf}$ ) are determined based on the 3D stress state of concrete plasticity proposed by Willam and Warnke [23]. These values are described below by substituting  $f_{lxe}$  and  $f_{lye}$  as the lateral confining pressures for the core, and  $f_{lxf}$  and  $f_{lyf}$  as the lateral confining pressures for the cover, respectively. Accordingly, the maximum compressive strength of confined concrete ( $f_{cc}$ ) under pure axial loads is obtained through the following steps.

- 1) Determine  $f_{lx}$  and  $f_{ly}$  for the concrete core and cover as previously mentioned. These values are then converted into negative numbers, corresponding to the major and intermediate principal stresses  $(\sigma_1, \sigma_2)$ , ensuring that  $\sigma_1 > \sigma_2$  is maintained.
- 2) Estimate the confined compressive strength of concrete ( $f_{cc}$ ), which corresponds to  $\sigma_3$ , the minor principal stress.
- 3) Determine the octahedral axial stress ( $\sigma_{oct}$ ), octahedral transverse stress ( $\tau_{oct}$ ), and the Lode angle ( $\theta$ ) by applying the equations provided below:

$$\sigma_{oct} = \frac{1}{3} [\sigma_1 + \sigma_2 + \sigma_3] \tag{44}$$

$$\tau_{oct} = \frac{1}{3}\sqrt{(\sigma_1 - \sigma_2)^2 + (\sigma_2 - \sigma_3)^2 + (\sigma_1 - \sigma_3)^2}$$
 (45)

$$\cos\theta = \frac{\sigma_1 - \sigma_{oct}}{\sqrt{2}\tau_{oct}} \tag{46}$$

4) Compute the ultimate stress Meridiam ( $\theta$ =0) and C ( $\theta$ =60 $\circ$ ) using the updated equations for the bilinear curves given in the formulas below.

If 
$$|\overline{\sigma_{oct}}| < 0.33$$
  $C = 0.107795 - 1.09083\overline{\sigma_{oct}}$  (47)

Other 
$$C = 0.336883 - 0.40357\overline{\sigma_{oct}}$$
 (48)

If 
$$|\overline{\sigma_{oct}}| < 0.767$$
 
$$T = 0.061898 - 0.62637\overline{\sigma_{oct}}$$
 (49)

Other 
$$T = 0.229132 - 0.40824\overline{\sigma_{oct}}$$
 (50)

where  $\overline{\sigma_{oct}} = \frac{\sigma_{oct}}{f_c}$ 

5) Compute the octahedral shear stress ( $\tau_{oct}$ ) using the interpolation function developed by Willam and Warnke.

$$\overline{\tau_{oct}} = C \frac{\frac{D}{2\cos\theta} + (2T - C)\sqrt{(D + 5T^2 - 4TC)}}{D + (2T - C)^2}$$
(51)

$$D = 4(C^{2} - T^{2})\cos^{2}\theta$$

$$\tau_{oct} = \overline{\tau_{oct}} \times f_{co}$$
(52)

6) Calculate the confined compressive strength of concrete for core and cover ( $f_{cce}$ ,  $f_{ccf}$ ) using the following equation:

$$f_{cc} = \sigma_3 = \frac{\sigma_1 + \sigma_2}{2} - \sqrt{4.5\tau_{oct}^2 - 0.75(\sigma_1 - \sigma_2)^2}$$
 (53)

for calculation of  $f_{cce}$  and  $f_{ccf}$  uses the trial-and-error method, and the obtained value is repeated in three or more stages until it reaches its actual value.

#### 3.4. Nominal axial load capacity of RC columns

According to loading types, RC columns are divided into two major categories: axially loaded and non-axially loaded columns. When external loads act on the center of a cross-section of columns, the column is axially loaded, and the normal axial stresses act on the cross-section of the column. The theoretical axial load capacity of unconfined concrete columns is obtained based on ACI-318-08 as follows [11]:

$$P_o = \alpha [0.85 f_{co} (A_g - A_{st}) + A_{st} f_v]$$
 (54)

When axially loaded RC columns are confined with FRP wraps, the maximum theoretical axial load capacity is obtained by the recommendations of ACI-440.2R-08 as follows:

$$P_n = \alpha [0.85 f_{cc} (A_q - A_{st}) + A_{st} f_v]$$
 (55)

When axially loaded RC columns are confined with combined confinement of FRP and TSR, the maximum confined axial load is obtained by the recommendations of ACI-440.2R-08 as follows [4]:

$$P_n = \alpha \left[ 0.85 f_{cce} (A_c - A_{st}) + 0.85 f_{ccf} (A_q - A_c) + A_{st} f_v \right]$$
 (55)

where  $\alpha$  is the accidental eccentricity factor, with  $\alpha=0.8$  for tied columns and  $\alpha=0.85$  for spiral columns.  $P_o$  and  $P_n$  are the theoretical axial load capacities of unconfined and confined RC columns, respectively.  $F_{cc}$  is the confined compressive strength of concrete retrofitted with FRP wraps,  $A_g$  is the gross area of the cross-section,  $A_{st}$  and  $f_y$  are the total area of longitudinal steel reinforcement and the tensile yield strength of the bars, respectively.  $F_{co}$  is the unconfined compressive strength of concrete, and  $f_{cce}$  and  $f_{cct}$  are the confinement compressive strength of the concrete core and cover, respectively.

#### 4. Results

#### 4.1. Parametric study of confined RC columns

In this study, five reinforced concrete columns with different characteristics were investigated. Four columns have 10φ20 and one of them has 10φ20 longitudinal reinforcement, and the stirrup diameter is 10 mm for each. The tensile yield strength of the longitudinal bars and transverse steel reinforcement is 420 MPa. The unconfined compressive strength and elastic modulus of the concrete are 25 MPa and 23500 MPa, respectively, while the unconfined compressive strain of the concrete is 0.2%. The modulus of elasticity for the steel reinforcement and the fiber-reinforced polymer are 200 GPa and 230 GPa, respectively, with the ultimate tensile strain of the FRP composite being 1.52%. The clear cover spacing is 25 mm for all crosssections, and the thickness of FRP ply is 0. 125 mm. The number of FRP layers, the corner rounding radius, and the TSR spacing vary for each cross-section. These parameters were studied to evaluate the stress-strain behavior, lateral confining pressures, confined compressive strength and strain of the concrete, and the theoretical axial load capacity of confined RC columns. Each parameter was evaluated individually for each cross-section with different properties. The main objectives of this study are to understand the structural behavior of confined reinforced concrete columns under varying levels of confinement subjected to pure axial loads. The first column has a rectangular cross-section with dimensions of 350 mm × 700 mm and an aspect ratio of b/h = 0.5. The second column also has a rectangular cross-section with dimensions of  $300 \times 600$ mm and an aspect ratio of b/h = 0.5. The third column has a rectangular cross-section with dimensions of  $350 \times 500$  mm and an aspect ratio of b/h = 0.7. The fourth and fifth columns have square cross-sections with an aspect ratio of b/h = 1, as shown in Fig. 9. All columns were analyzed analytically under axial loads with various parameters.

The results of a parametric study of five reinforced concrete columns retrofitted with an FRP jacket and lateral steel reinforcement are shown in Table 4. In this table, all parameters of the columns' cross-sections were evaluated using the Lam and Teng model, the Mander et al. [14] model, and the Willam and Warnke [23] 3D stress state model, as these models have high accuracy for FRP- and TSR-confined RC columns. For all cross sections, the confined compressive strength and strain of concrete, as well as the theoretical axial load capacity, were calculated based on the number of FRP layers and the corner radius.

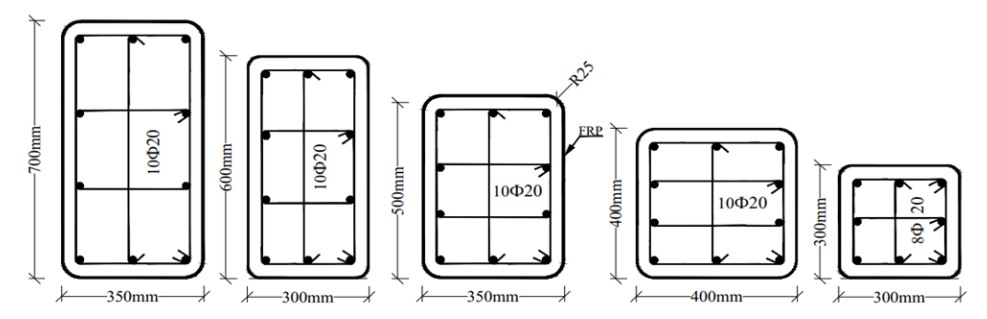


Fig. 9. Confined column cross-sections for the analytical study

Table 2. Properties of cross-sections

Property	Value	Property	Value
F <sub>co</sub> (MPa)	25	E <sub>f</sub> (MPa)	230000
F <sub>y</sub> (MPa)	420	$t_f$ (mm)	0.125
F <sub>ys</sub> (MPa)	420	$\epsilon_{ m fu}$	0.018
CC (mm)	25	$\epsilon_{ m fe}$	0.0089
d <sub>b</sub> (mm)	20	$A_s (mm^2)$	3140
$d_s$ (mm)	10	$A_t (mm^2)$	78.5
S (mm)	150	b×h (mm)	350×500
R (mm)	25	b×h (mm)	300×600
E <sub>s</sub> (MPa)	2×10 <sup>5</sup>	b×h (mm)	400×400

Table 3. Details of cross-sections and longitudinal reinforcement

Section (mm)	d <sub>b</sub> (mm)	d <sub>s</sub> (mm)	Bars in x	Bars in y	<b>f</b> g (%)
350×500	20	10	3	4	1.80
300×600	20	10	3	4	1.74
400×400	20	10	3	4	1.96
350×700	20	10	3	4	1.28
300×300	20	10	3	3	2.09

The study shows that the structural axial behavior of reinforced concrete columns improves with an increase in the number of FRP ply layers. According to the analytical study, each layer of FRP wraps increases the axial load capacity by at least 2.7%, ductility by 30%, and confined compressive strength of concrete by 3.7%.

Additionally, a decrease in the corner radius improves performance; calculations show that every 10 mm increase in corner radius improves the confined strength of concrete by 1.5% and ductility by 8.7%. Furthermore, the aspect ratios of the cross sections play a significant role in the strength and ductility of the columns. If the dimension ratio or width-to-height ratio is close, the axial capacity increases; if they are very different, the strength and ductility decrease. Notably, square cross sections are more efficient than other rectangular sections. Statistics show that FRP significantly increases the axial strength of columns compared to unconfined concrete.

The analytical results of five reinforced concrete columns strengthened with combined confinement of FRP/TSR are presented in Table 5. All parameters of the cross-section were evaluated by combining Mander et al.'s [14] model for TSR confinement and Lam and Teng's model for FRP wraps. The value of the confined compressive strength of the concrete was obtained using the 3D state-stress method that was developed by Willam and Warnke, and the procedure was carried out using a trial-and-error approach. In this type of confinement, the confined compressive strength and strain of the concrete column are calculated separately for the core and the cover, as both have different values. Based on the lateral confining pressures, the theoretical axial load capacity is calculated. The results show that the combined confinement with carbon fiber reinforced polymer (CFRP) and transverse steel reinforcement (TSR) provides more advantages than the single FRP ply confinement. For the five reinforced concrete columns, the combined confinement increases the axial load capacity by 10% more than the single confinement or FRP wraps, on average.

Table 4. Results of the analytical study on FRP confinement

Section mm	$N_{\mathrm{f}}$	F <sub>cc</sub> (MPa)	%in	Eccu %	%in	P <sub>n</sub> (kN)	%in	R <sub>c</sub> (mm)	F <sub>cc</sub> (MPa)	%in	$\mathcal{E}_{ccu}$	%in
	0	25.00	0	0.35	0	3977	0	0	26.54	0	0.58	0
	1	25.76	3.04	0.46	31.42	4066	2.24	10	26.85	1.17	0.62	6.89
350×500	2	26.53	6.12	0.58	65.71	4155	4.48	15	27.00	1.73	0.65	12.07
	3	27.30	9.20	0.69	97.14	4245	6.74	20	27.15	2.30	0.67	15.51
	4	28.06	12.24	0.80	128.50	4334	8.98	25	27.30	2.86	0.69	18.96
	0	25.00	0	0.35	0	4062	0	0	25.96	0	0.68	0
	1	25.36	1.44	0.47	34.28	4107	1.12	10	26.15	0.73	0.75	10.29
300×600	2	25.71	2.84	0.59	68.57	4147	2.11	20	26.34	1.46	0.81	19.11
	3	26.07	4.28	0.72	105.7.	4191	3.16	30	26.51	2.12	0.87	27.94
	4	26.43	5.72	0.84	140.00	4234	4.23	40	26.67	2.73	0.93	36.76

Table 4. Continued

Section mm	$N_{\mathrm{f}}$	F <sub>cc</sub> (MPa)	%in	Eccu %	%in	P <sub>n</sub> (kN)	%in	R <sub>c</sub> (mm)	F <sub>cc</sub> (MPa)	%in	$\mathcal{E}_{ccu}$	%in
	0	25.00	0	0.35	0	3722	0	0	28.39	0	0.55	0
	1	26.69	6.76	0.45	28.57	3903	4.86	10	29.10	2.50	0.60	9.09
400×400	2	28.39	13.56	0.56	60.00	4084	9.72	20	29.76	4.82	0.64	16.36
	3	30.08	20.32	0.66	88.57	4246	14.1	30	30.40	7.08	0.68	23.63
	4	31.78	27.12	0.76	117.1	4445	19.4	40	31.00	9.20	0.72	30.90
	0	25	0	0.35	0	5167	0	0	25.62	0	0.56	0
250 700	2	25.59	2.36	0.52	48.57	5264	1.87	15	26.04	1.64	0.71	26.78
350×700	3	25.88	3.52	0.66	88.57	5312	2.81	20	26.11	1.91	0.73	30.35
	4	26.18	4.72	0.76	117.1	5360	3.74	25	26.18	2.18	0.76	35.71
	0	25	0	0.35	0	2131	0	0	29.52	0	0.63	0
300×300	2	29.97	19.88	0.65	85.71	2429	13.9	15	31.35	6.20	0.74	17.46
	3	32.46	29.84	0.80	128.57	2578	20.9	20	31.91	8.09	0.77	22.22
	4	34.95	39.8	0.96	174.28	2727	27.9	25	32.46	9.96	0.80	26.98

Table 5. Parametric study results for combined FRP and TSR confinement

Section, mm	nm 350×500			300×600			400×400			350×700		
$N_{\mathrm{f}}$	1	3	4	2	3	4	1	2	3	3	4	5
$F_{lf}\!/F_{co}$	0.028	0.084	0.112	0.058	0.087	0.116	0.03	0.06	0.087	0.071	0.095	0.12
F <sub>cce</sub> (MPa)	29.08	32.08	33.62	30.4	31.87	33.32	28.9	30.39	31.87	29.68	30.90	32.11
F <sub>ccf</sub> (MPa)	26.53	29.49	31.06	28.12	29.6	31.07	26.6	28.07	29.6	28.82	30.03	30.26
$P_n(kN)$	4371	4725	4900	4633	4811	4986	4097	4267	4438	5914	6115	6313
R <sub>c</sub> (mm)	5	15	30	5	15	30	5	15	30	20	30	40
$F_{lf}\!/F_{co}$	0.02	0.07	0.12	0.04	0.07	0.12	0.02	0.05	0.09	0.067	0.10	0.14
Fcce (MPa)	27.16	30.02	32.46	28.21	29.93	32.31	27.24	28.85	31.15	29.48	31.17	33.05
F <sub>ccf</sub> (MPa)	26.14	29.0	31.44	27.32	29.05	31.44	26.17	27.78	30.08	28.61	30.31	32.22
$P_n\left(kN\right)$	4207	4541	4826	4427	4634	4920	3939	4110	4355	5880	6158	6467

All stirrups \phi10@250mm c/c, f<sub>ys</sub>=420MPa

# 4.2. Parametric study of confined RC columns

The stress-strain curves for the confined RC columns with three types of confinement configurations are shown in Fig. 10. for two confined RC columns that are strengthened with FRP, TSR, and combined confinement or both. The first four curves illustrate the comparison of FRP, TSR, and FRP&TSR

confinement for rectangular cross-sections. The first and second curves (10-a and 10-b) show the comparison of three types of confinement configurations for 350×500 mm and 350×700 mm RC columns. According to the curves, the combined confinement technique has significant advantages over the individual techniques in enhancing the cross-sectional strength and ductility of axially loaded columns. The third and fourth curves (10-c and 10-d) present the axial stress-strain relationships for FRP confinement (F<sub>lam</sub>), which represents the axial compressive stress of concrete confined by FRP, and the combined confinement method with FRP&TSR. For the combined confinement, the stress-strain relationships are evaluated separately for the core and cover of rectangular columns. The variables  $f_{ccf}$  and  $F_{cce}$  represent the confined compressive axial stress of concrete for the core and cover, respectively. The stress-strain relationships are shown for 350×500 mm and 300×600 mm rectangular cross-sections. Based on the curves, the combined FRP & TSR confinement increases the strength of RC columns compared to single-ply FRP, although its ductility is lower than that of FRP confinement. The fifth curve (10-e) shows the stress-strain relationships based on various FRP layer configurations for a 300×600 mm cross-section of the column. Based on the curves, additional layers have a significant effect on enhancing the concrete strength and ductility. The last curves (10-f) show the stress-strain relationships for TSR confinement based on stirrup spacings of s = 150 mm and s = 300 mm. The curves were obtained according to the Mander et al. [14] model for a rectangular 350×500 mm column. According to the graph, the TSR spacing has a significant effect on the strength and ductility of concentrically loaded columns.

The peak or maximum confined compressive strength of concrete, in relation to TSR spacing, the number of FRP layers, and the rounded corner radius of rectangular cross-sections, is illustrated in Fig. 11. All these factors were investigated analytically under uniaxial loads for rectangular RC columns. The first graph (11-a) shows the relationship between  $F_{cc}$  and stirrup spacing, calculated for various spacings in  $350 \times 500$  mm RC columns. According to the graph, an increase in TSR spacing significantly decreases the confined strength of the column cross-section under axial load. The second and third graphs (11-b and 11-c) illustrate the values of  $F_{cc}$  based on the number of FRP layers in the combined confinement technique for rectangular and square RC columns. Based on the results, a greater number of FRP plies dramatically enhances the axial strength capacity and deformability of the column cross-sections. The final graph (11-d) presents the effect of the rounded corner radius of a  $400 \times 400$  mm cross-section on the compressive strength of a concrete column. According to the curve, a larger corner radius increases both the strength and ductility of FRP-confined columns under axial loading.

The effect of the rounded corner radius of rectangular/square cross-sections on the axial strength capacity and ductility of RC columns strengthened with FRP wraps is illustrated for various cross-sections in Fig. 12. The effect of corner radius on FRP-confined RC columns is substantial, as it immediately influences the mechanical behavior of the FRP jackets. It distributes stress variations uniformly around the cross-section, while sharp corners can create stress concentrations in the FRP wraps due to localized strain. A larger corner radius enhances the efficiency of the FRP jacket because the wraps adhere better to the column's exterior surfaces. The following stress and strain behaviors are investigated for different rounded corner radii. Based on the curves, a larger radius remarkably increases the axial compressive strength of rectangular columns externally strengthened with FRP wraps.

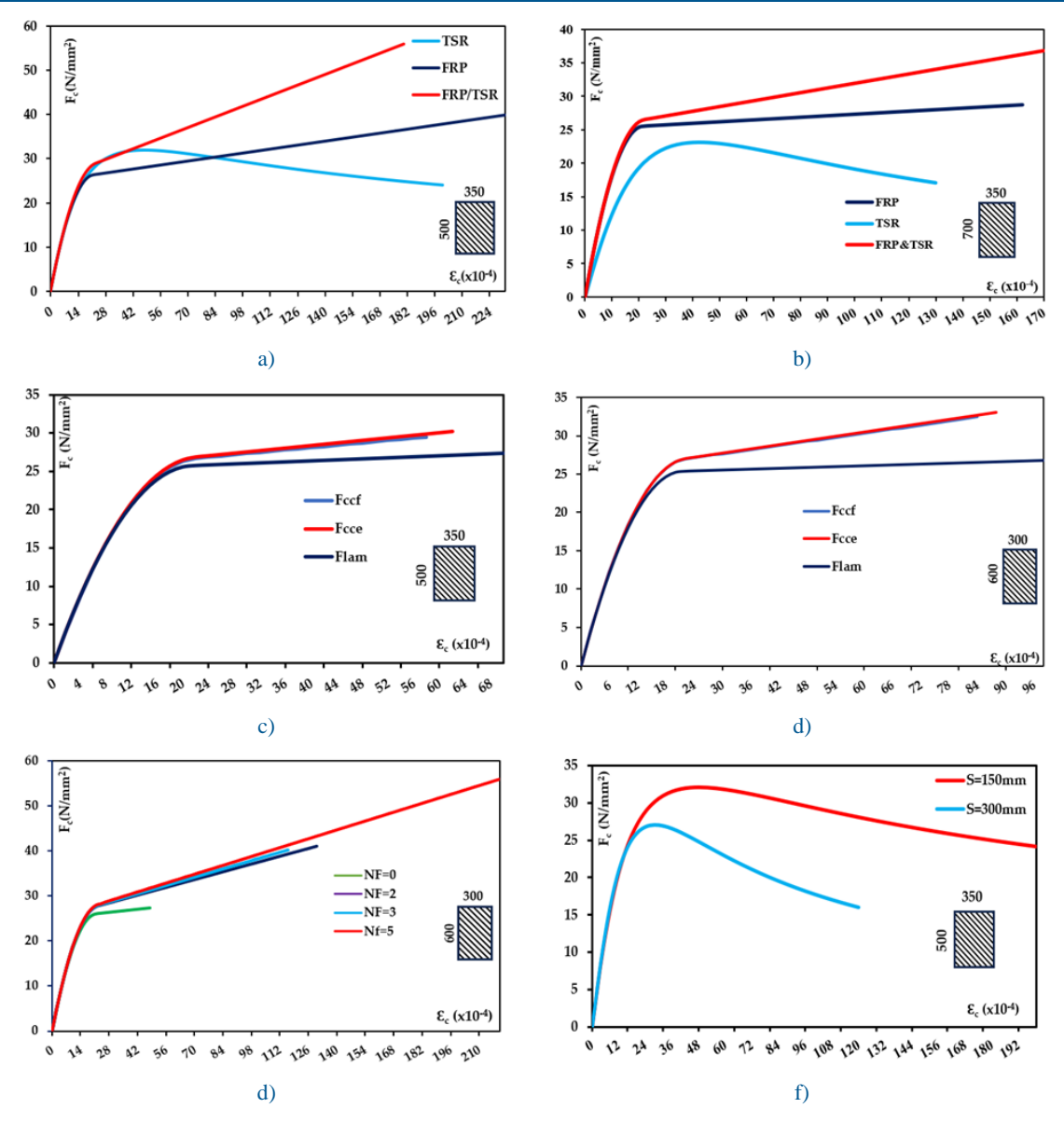


Fig. 10. Stress-strain curves: a) and b) Comparison of FRP, TSR, and FRP&TSR confinements, c) and d) FRP and FRP&TSR confinement, e) Based on the number of FRP layers, f) Based on TSR spacing

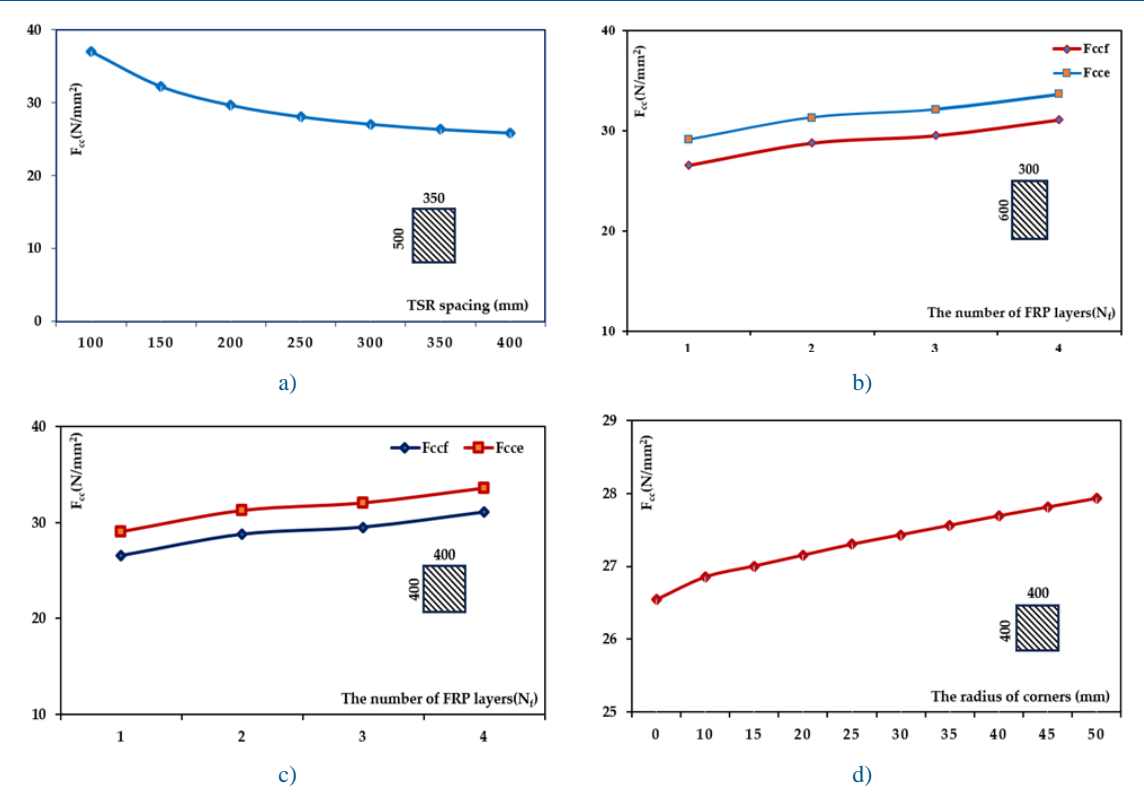


Fig. 11. Peak compressive strength of concrete: a) Based on TSR spacing, b) According to FRP plies, c) Based on the number of FRP layers, d) According to corner radius

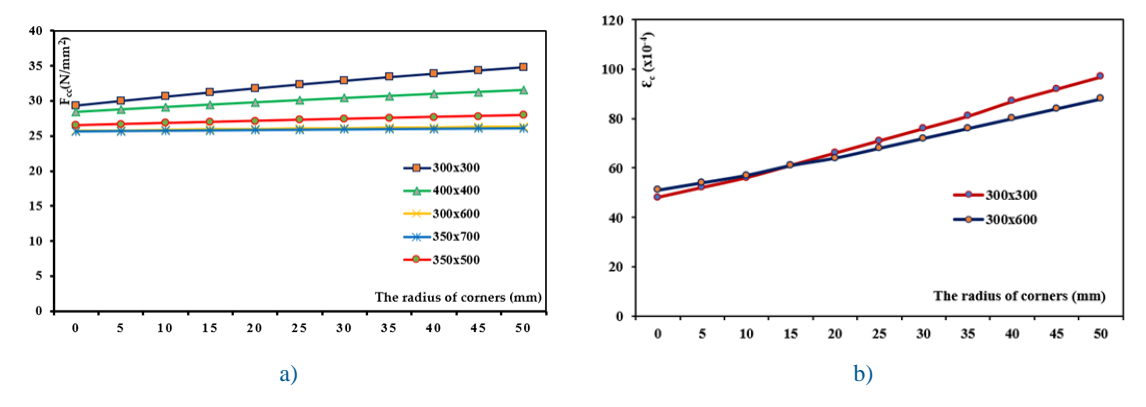


Fig. 12. Peak confined compressive strength and strain: a) Stress as a function of corner radius, b) Strain as a function of corner radius

#### 4.3. Calculation of theoretical axial load capacity

For a more detailed analysis, the first cross-section of the rectangular column  $350 \times 500$  mm, based on the FRP thickness, was analyzed in three stages: unconfined, FRP-confined, and combined FRP and TSR confinement. The values of  $f_{cce}$  and  $f_{ccf}$  were determined using an Excel sheet and calculated according to the 3D stress-state procedure [23]. The calculation steps for the theoretical axial load capacities under all conditions are outlined step-by-step in the following tables [11].

Table 6. Extracted parameters for analysis

Section mm		350×500							
$N_{ m f}$	1	2	3	4					
$F_{\mathrm{lf}}/F_{\mathrm{co}}$	0.03	0.06	0.08	0.11					
F <sub>cce</sub> (MPa)	29.08	30.60	32.10	33.62					
F <sub>ccf</sub> (MPa)	26.53	28.05	29.57	31.08					

Table 7. Comparison of analytical study

$N_{\mathrm{f}}$	P <sub>0</sub> =3976.6 kN	P <sub>n</sub> (kN)	%in
1	FRP	4066	2.25
1	FRP&TSR	4371.3	9.92
2	FRP	4155.3	4.49
2	FRP&TSR	4548.78	14.38
3	FRP	4244.6	6.74
3	FRP&TSR	4725.9	18.84
4	FRP	4334	8.98
4	FRP&TSR	4902.1	23.27

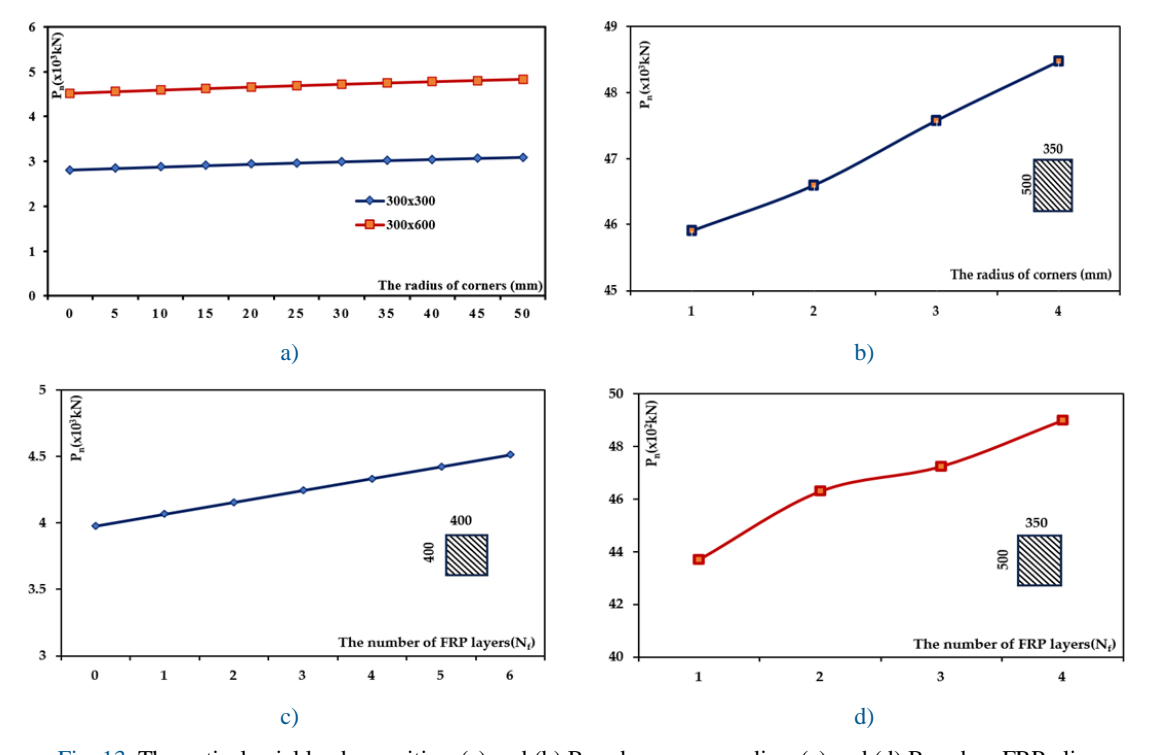


Fig. 13. Theoretical axial load capacities: (a) and (b) Based on corner radius, (c) and (d) Based on FRP plies

The theoretical axial load capacities derived from the confinement applications based on FRP thickness are presented in Table 7. Both FRP wrap confinement and the FRP/TSR technique were compared to the unconfined state. The results highlight the greater effectiveness of combined confinement compared to single or FRP-only confinement. According to the analytical calculations, FRP confinement increases the axial load capacity of columns by an average of 5.61% compared to unconfined RC columns, while combined confinement enhances the axial load capacity by 16.6% compared to the unconfined state. When comparing combined confinement to FRP single confinement, the results show an average increase of 10.98%.

The theoretical axial load capacities of confined RC columns, investigated using analytical models, are shown in Fig. 13. These results are compared based on the number of FRP plies and the corner radius, with all parametric variations analyzed for different section types and confinement configurations. Figs. 13-a and 13-b illustrate the nominal axial load values as a function of the corner radius for three confined rectangular RC columns. Based on the graphs, the axial load capacity increases considerably with an increase in the corner radius under pure compression loads. Figs. 13-c and 13-d present the relationship between the axial load capacity of the RC columns and FRP thickness, calculated for two cross-sections and two types of confinement configurations.

#### 4.4. Comparison of analytical and experimental studies

The comparison between the analytical study and experimental data, as shown in Tables 8-9, is based on findings from the literature. Eid and Paultre [12] tested several square and rectangular columns strengthened with FRP and combined FRP/TSR. All columns were reinforced with four longitudinal bars of 8 mm diameter, corresponding to a longitudinal steel percentage of  $\rho_g$ =0.89%. The transverse steel reinforcement consisted of stirrups with a 6 mm diameter, spaced at 100 mm and 50 mm intervals. The tensile yield strengths of the longitudinal steel bars and stirrups were 513 MPa and 258 MPa, respectively. The unconfined compressive strength of the concrete was 33.7 MPa, 41.5 MPa, and 78.2 MPa. The concrete mix was prepared and delivered by a batch plant, with a water-cement ratio of 0.5, dolomite aggregates of maximum sizes 14 mm and 9.5 mm, a density of 2389 kg/m³, an air content of 3%, and a slump of 90 mm. To determine the average compressive strength, three concrete cylinders (150 mm in diameter and 300 mm in height) were tested under uniaxial loading.

For external confinement, carbon fiber-reinforced polymer (CFRP) jackets with a ply thickness of 0.381 mm were used. The reinforced concrete specimens were wrapped with either two or four layers of FRP. The mechanical properties of the linear-elastic FRP composite, as provided by the manufacturer, include an elastic modulus of  $E_f$ =65.4 GPa, an ultimate tensile strength of  $f_{fu}$ =894 MPa, and an ultimate tensile strain of  $\varepsilon_{fu}$ =0.0133. All physical and mechanical details of the experimental specimens are shown in Table 8, such as cross-sectional aspect ratios, unconfined compressive strength of concrete, FRP jacket properties, and TSR mechanical specifications.

For greater accuracy, the comparison of analytical and experimental studies of axial compressive stress-strain curves is presented in Fig. 14. The comparison includes an RC column specimen with dimensions of 150×150 mm, confined by combined FRP and TSR configurations, and a 150×225 mm specimen confined solely with FRP jackets. The results show a close agreement between the confined compressive strength and ductility of RC columns obtained from the analytical studies and the experimental data.

The results of the analytical studies, which were investigated using models, are compared with the results of experimental works taken from the literature and summarized in Table 9. Based on the findings, the analytical values of the peak confined compressive strength of concrete show close agreement with the values obtained from the test results. However, the values of the maximum confined compressive strain of concrete differ slightly, depending on various factors such as material property variability in FRP RC columns, simplified assumptions in the analytical models, testing setup, instrumentation issues, and others.

The statistical method of regression is used to compare the peak confined compressive strength of concrete obtained from analytical models and experimental data in confined column specimens, as illustrated in Fig. 15. The first graph shows the direct relationship between the analytical  $F_{cc}$  and experimental  $F_{cc}$  for specimens confined with FRP confinement and combined FRP & TSR confinement techniques. The value of  $R^2$ =96% has been evaluated, indicating a high degree of agreement between the two sets of data, or a very strong correlation between the analytical and experimental results. The second regression presents the values of normalized analytical  $F_{cc}/F_{co}$  and experimental  $F_{cc}/F_{co}$  for column specimens, and the correlation between the data is 84%, indicating that the analytical models are relatively effective in comparison with the experimental data.

Table 8. Properties of the experimental specimens

			_		FRP			TSR	
Specimen numbers	b×h (mm×mm)	R <sub>c</sub> (mm)	F <sub>co</sub> (MPa)	t <sub>f</sub> (mm)	E <sub>f</sub> (GPa)	$\epsilon_{\rm fu} \\ \%$	F <sub>ys</sub> (MPa)	S (mm)	ds (mm)
C30S100N2	150×150	15	33.7	0.762	65.4	1.33	258	100	6
C30S50N2	150×150	15	33.7	0.762	65.4	1.33	258	50	6
R4R25	150×225	25	41.5	0.66	257	1.76	-	-	-
C30S50N4	150×150	15	33.7	1.524	65.4	1.33	258	50	6
C30S100N4	150×150	15	33.7	1.524	65.4	1.33	258	100	6
1R-2.0	150×300	30	35.3	0.167	229	1.84	-	-	-
A20R30L5	112.5×225	30	78.2	0.702	240	1.55	-	-	-
A20R30L3	112.5×225	30	78.2	0.702	240	1.55	-	-	-
A15R30L3	125.5×187.5	30	77.2	0.702	240	1.55	-	-	-
A15R3L5	125×187.5	30	79.6	1.17	240	1.55	-	-	-

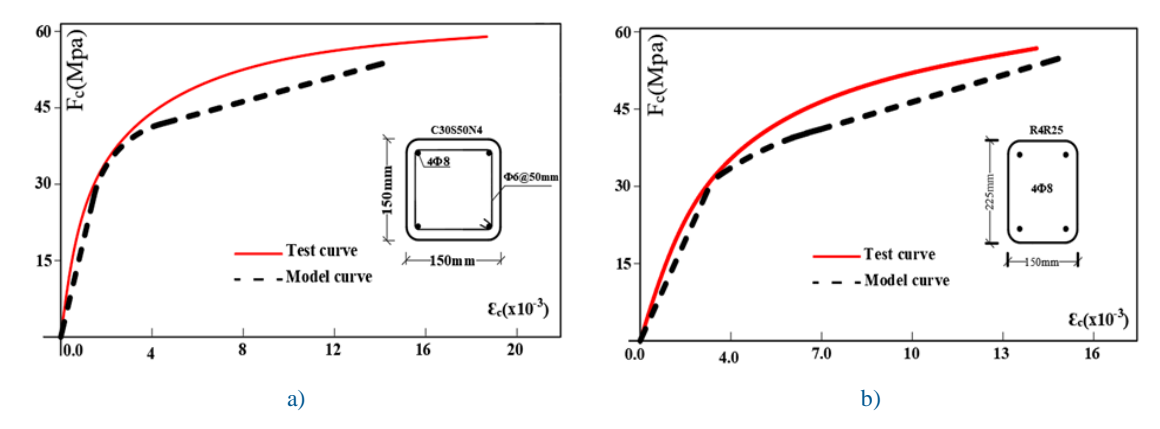


Fig. 14. Comparison of analytical and experimental data: (a) Combined confinement, (b) FRP confinement

$T_{\alpha}$	bla	0 0	omparison	of av	narima	ntal data	and	analytical	etudios
- 1 2	ınıe	9. U.	ombarison	or ex	nerime	ntai data	ı ana	anaivucai	studies

			$f_{cc}$		$\mathcal{E}_{\mathrm{cc}}$			
Specimen number	b×h (mm×mm)	Exp. (MPa)	Model (MPa)	Dif. %	Exp.	Model %	Dif. %	
C30S100N2	150×150	39.9	40.92	2.55	1.06	0.59	44.3	
C30S50N2	150×150	44.8	45.76	2.14	1.21	0.86	28.9	
R4R25	150×225	51.9	51.62	0.54	1.04	1.3	25	
C30S50N4	150×150	57.5	52.2	9.2	1.87	0.98	47.5	
C30S100N4	150×150	57.1	48.11	15.7	1.2	0.84	30	
1R-2.0	150×300	37.44	35.43	5.36	0.82	0.38	53.6	
A20R30L5	112.5×225	84.3	85.68	1.62	1.63	1.13	30.6	
A20R30L3	112.5×225	78.4	85.35	8.84	1.47	1.09	25.85	
A15R30L3	125.5×187.5	81.3	91.5	12.54	1.03	1.08	4.85	
A15R3L5	125×187.5	95.8	103.43	7.96	1.62	1.53	5.55	

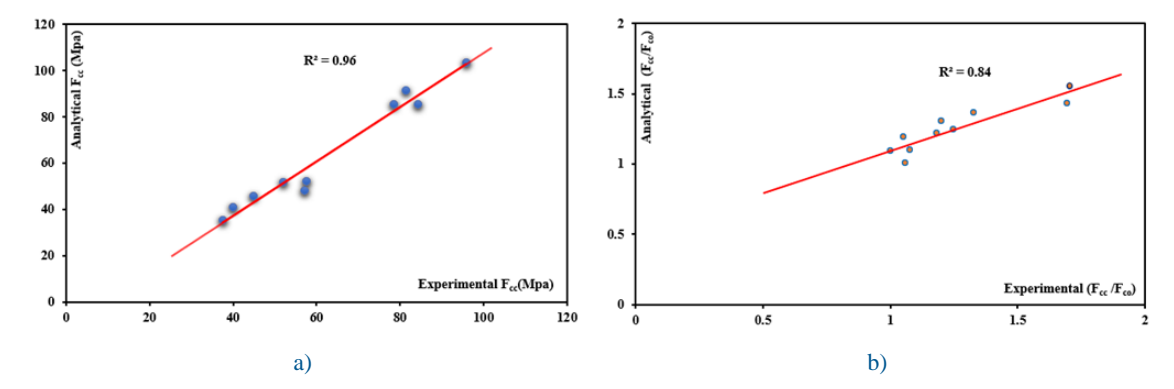


Fig. 15. Comparison of analytical and experimental data: a) Peak confined stresses, b) Normalized confined axial stress

#### 5. Conclusions

This study investigates the analytical behavior of rectangular reinforced concrete columns externally strengthened with fiber-reinforced polymer (FRP) jackets and internally reinforced with transverse steel reinforcement (TSR) or stirrups under axial compressive loads. Based on experimental data and previous studies, suitable models for predicting the structural behavior of RC columns under combined confinement have been identified. The Lam and Teng model have been determined to be the most accurate for RC columns retrofitted with FRP, while the Mander model demonstrates high accuracy for RC structures confined with TSR. In this study, a combination of both models was employed to evaluate the performance of RC columns subjected to axial loads. Additionally, the maximum confined compressive strength of concrete was determined using the three-dimensional state of stress developed by Willam and Warnke for combined confinement conditions.

The role of cross-sectional properties and material mechanical properties was evaluated for at least five rectangular RC columns to analyze the precise axial structural behavior of combined confined RC columns. Parameters such as the confined compressive strength and strain of concrete, confinement ratio, and

theoretical axial load capacities of the columns were determined. Their effects were illustrated and analyzed through stress-strain curves, tables, and graphs. Furthermore, ten rectangular and square FRP and combined FRP/TSR experimental specimens were selected from the literature for comparison.

All specimens were analyzed analytically using the proposed models, and the results were compared with experimental data. The findings were presented in tables and graphs, demonstrating a close agreement between the selected models and the experimental studies based on the obtained values. Finally, the study demonstrates the significant potential of combined confinement in improving the structural behavior of rectangular RC columns under axial loading. It identifies acceptable levels of strength, ductility, and capacity. This method of analysis provides valuable insights into the field of structural engineering and retrofitting techniques.

## Conflict of interests

The author(s) declared no potential conflicts of interest with respect to the research, authorship, and/or publication of this article.

# **Funding**

This research received no external funding.

# Data availability statement

Data generated during the current study are available from the corresponding author upon reasonable request.

#### Nomenclature

Symbol	Description	Symbol	Description
FRP	Fiber reinforced polymer	$k_a,k_b$	Strength and strain efficiency factor
TSR	Transverse steel reinforcement	$k_{\rm e}$	Confinement effectiveness coefficient
$A_{t}$	Cross sectional area of stirrups	$\mathbf{K}_0$	Unconfined concrete strength factor
$A_s$	Cross-sectional area of longitudinal bars	$k_h,k_v$	Horizontal and vertical confinement effectiveness coefficient
$b_{c,} h_{c}$	Column's cross section dimensions of core	$K_{1,}K_{2}$	Lateral confinement and load interaction factor or FRP confinement factors
b, h	Column's cross section dimensions, b≤h	$n_{\rm f}$ , $t_{\rm f}$	The number and thickness of FRP layers
Ac	Area of effectively confined concrete core	$\psi_{\rm f}$	Additional reduction factor
$A_{\rm e}$	Effective area of confined concrete	$\mathbf{P}_{\mathbf{n}}$	Nominal axial strength of RC columns
$A_{g}$	Gross area of cross section	φ	Resistance factor
D	Equivalent cross-sectional diameter	$\mathbf{f}_{\mathrm{g}}$	Steel percentage of cross section
Acc	The area of concrete within the center line of the Perimeter hoop	$f_{cc}$	The ratio or longitudinal reinforcement area to the area of concrete core
cc	Clear cover spacing	$\mathcal{F}_{\mathrm{s}}$	Ratio of the volume of transverse confining steel to the volume of confined concrete
$R_c$	Corner radius of the rectangular cross-section	$\mathbf{f}_{x}, \mathbf{f}_{y}$	The ratio of stirrup reinforcement to the confining concrete in the x and y-direction

W'	Clear distance between longitudinal bars	$\epsilon_{ m co}$	Strain of unconfined concrete
S, S'	Center-to-center and clear spacing of stirrups	$\epsilon_{\rm cc}$	The maximum confinement axial compressive strain
$E_{c},E_{s}$	Elastic modulus of concrete and steel reinforcement	$\epsilon_{\rm cce},\epsilon_{\rm ccf}$	The maximum confinement axial compressive strength of the concrete in the core and cover
$E_{\rm f}$	Elastic modulus of FRP	$\epsilon_{\mathrm{cu}}$	Maximum concrete strain value
$E_2$	Linear slope of the stress-strain curve	$\epsilon_{\rm c}$	Axial strain of concrete
$E_{\text{sec}}$	The ratio of confined concrete stress to strain	$\epsilon_{\mathrm{fu}}$	Maximum FRP tensile strain
Fco, f'c	Unconfined compressive strength of concrete	$\epsilon_{\mathrm{fe}}$	The reduced FRP tensile strain
$f_c$	Axial stress of concrete	$\epsilon_{ m lo}$	TSR strain
$\mathbf{f}_{t}$	Transition axial stress of concrete	$\epsilon_{t}$	Transition strain of curve
$f_{cc}$	Maximum confined compressive strength of concrete	$G_1,G_2$	Principle stresses in x and y directions
$f_{\rm ccf}$	Maximum confined strength of the concrete cover	б <sub>3</sub>	Minor principal stress
$f_{\rm cce}$	Maximum confined strength of the concrete core	$\sigma_{oct}$	Octahedral axial stress
$f_l$	the confinement lateral pressure	$\tau_{\rm oct}$	Octahedral shear stress
$\mathbf{f}_{ ext{lf}}$	Lateral confinement pressure in the concrete cover	R	Correlation factor
$F_y$ , $F_{ys}$	Yield strength of longitudinal bars and stirrups	α	Accidental eccentricity factor

#### References

- [1] Soudki K, Alkhrdaji T (2005) Guide for the design and construction of externally bonded FRP systems for strengthening concrete structures (ACI 440.2R-02). Proceedings of the Structures Congress and Exposition. <a href="https://doi.org/10.1061/40753(171)159">https://doi.org/10.1061/40753(171)159</a>
- [2] Jiang T, Teng JG (2007) Analysis-oriented stress-strain models for FRP-confined concrete. Eng Struct 29:2968– 2986.
- [3] Koksal HO, Doran B, Turgay T (2009) A practical approach for modeling FRP wrapped concrete columns. Constr Build Mater 23:1429–1437.
- [4] Al-Rahmani A, Rasheed H (2016) Combined transverse steel-external FRP confinement model for rectangular reinforced concrete columns. Fibers. <a href="https://doi.org/10.3390/fib4010008">https://doi.org/10.3390/fib4010008</a>
- [5] Liao JJ, Zeng JJ, Zhuge Y, Zheng Y, Ma G, Zhang L (2023) FRP-confined concrete columns with a stress reduction-recovery behavior: A state-of-the-art review, design recommendations and model assessments. Compos Struct. <a href="https://doi.org/10.1016/j.compstruct.2023.117313">https://doi.org/10.1016/j.compstruct.2023.117313</a>
- [6] Lam L, Teng JG (2003) Design-oriented stress-strain model for FRP-confined concrete in rectangular columns. Journal of Reinforced Plastics and Composites 22(13):1149-1186. https://doi.org/10.1177/0731684403035429
- [7] Afifi MZ, Mohamed HM, Chaallal O, Benmokrane B (2014) Confinement model for concrete columns internally confined with carbon FRP spirals and hoops. Journal of Structural Engineering 141(9):04014219. https://doi.org/10.1061/(ASCE)ST.1943-541X.0001197
- [8] Wei Y, Xu Y, Wang G, Cheng X, Li G (2022) Influence of the cross-sectional shape and corner radius on the compressive behaviour of concrete columns confined by FRP and stirrups. Polymers (Basel). https://doi.org/10.3390/polym14020341

- [9] Samaan M, Mirmiran A, Shahawy M. (1998) Model of concrete confined by fiber composites. J Struct Eng.124(9):1025–31.
- [10] Mirmiran A, Shahawy M. (1997) Behavior of concrete columns confined by fiber composites. J Struct Eng.123(5):583-90.
- [11] ACI 440.2R-08: Guide for the Design and Construction of Externally Bonded FRP Systems for Strengthening Existing Structures. ACI Committee 440, American Concrete Institute, Farmington Hills, 2008.
- [12] Eid R, Paultre P (2017) Compressive behavior of FRP-confined reinforced concrete columns. Eng Struct 132:518–530.
- [13] Rasheed HA (2014) Strengthening Design of Reinforced Concrete with FRP. CRC Press, Boca Raton. https://doi.org/10.1201/b17968
- [14] Mander JB, Priestley MJN, Park R. (1988) Theoretical stress–strain model for confined concrete. J Struct Eng.;114(8):1804–26.
- [15] Richart FE, Brandtzaeg A, Brown RL (1928) A Study of the Failure of Concrete under Combined Compressive Stresses. Engineering Experiment Station. University of Illinois Bulletin, No: 185.
- [16] Wang YC, Hsu K (2008) Design of FRP-wrapped reinforced concrete columns for enhancing axial load carrying capacity. Compos Struct 82:132–139.
- [17] Yang K, Yu T, Ma G, Zhao J, Sun S (2022) Study on the constitutive model of concrete confined by multi-spiral composite stirrups. Buildings 12(2):2179. https://doi.org/10.3390/buildings12122179
- [18] Teng JG, Xiao QG, Yu T, Lam L (2015) Three-dimensional finite element analysis of reinforced concrete columns with FRP and/or steel confinement. Eng Struct 97:15–28.
- [19] Harajli MH (2006) Axial stress-strain relationship for FRP confined circular and rectangular concrete columns. Cem Concr Compos 28:938–948.
- [20] Faustino P, Chastre C (2015) Analysis of load-strain models for RC square columns confined with CFRP. Compos B Eng 74:23–41.
- [21] Ilki A, Peker O, Karamuk E, Demir C, Kumbasar N. (2008) FRP retrofit of low and medium strength circular and rectangular reinforced concrete columns. J Mater Civ Eng. 20(2):169–88.
- [22] Pellegrino C, Modena C (2010) Analytical model for FRP confinement of concrete columns with and without internal steel reinforcement. Journal of Composites for Construction 14(6):693-705. https://doi.org/10.1061/(ASCE)CC.1943-5614.0000127
- [23] Willam KJ, Warnke EP. (1975) Constitutive model for the triaxial behavior of concrete. Proc Int Assoc Bridge Struct Eng. 19:1–30.